12

Synthesis and Sintering Studies of Magnesium Aluminum Silicate Glass Ceramic

Shahid-Khan Durrani*, Muhammad-Ashraf Hussain,
Khalid Saeed, Syed-Zahid Hussain, Muhammad Arif and Ather Saeed
Materials Division, Directorate of Technology, PINSTECH, P. O. Nilore, Islamabad, Pakistan

1. Introduction

1.1 Ceramic materials

Ceramic materials are complex compounds and containing both metallic and non-metallic elements. Typically, ceramics are very hard, brittle, high melting point materials with low electrical and thermal conductivity, good chemical and thermal stability, and high compressive strengths (Barsoum, 1997; Minh et al., 1995). Ceramics are of tremendous interest primarily because of their wide range of applications in high temperature environments; they are also extensively used in fuel technology (Koshiro et al, 1995), oxygen sensor (Ciacchi, et al. 1994), magnets ceramics (Valenzuela,2005) , all electronic equipments including integrated-chips, capacitors and digital alarms (Miller,& M. R. Miller (2002), telecommunication (Bhargava, A.K. 2005), abrasives (Callister, 2007) , ceramic crystal-glass (Carter, & Norton. (2007), ceramic insulators are widely used in the electrical power transmission system (Chowdhury, 2010), ceramic superconductors (David E. C.&, Brece K.Zoitos, 1992) and other pharmaceuticals industries (Rice, & R. W. Rice, (2002) etc.

Ceramic materials can be classified into four main groups (Rajendran, V. 2004):

i. The amorphous ceramics, which are generally referred to as "glasses".
ii. Crystalline ceramics**,** which are single phase materials like alumina, or mixtures of such materials.
iii. Bonded ceramics**,** where individual crystals are bonded together by a glassy matrix, such as clay products.
iv. Cements**,** these are crystalline, and also amorphous materials.

The structures of ceramics fall into two main groups:

- Simple crystal structures: containing ionic or covalent bonds, or a mixture of the two. Examples are magnesium oxide, which is an ionic compound with cubic structure, and silicon carbide, with covalent bonds and a tetrahedral structure like diamond. Alumina has a close packed hexagonal structure, with a mixture of covalent and ionic bonds,

* Corresponding Author

with one-third of the potential aluminum sites vacant in order to suit the valency requirements of the two elements ((Mostaghaci, H. 1996).

- Complex silicate structure**s:** The majority of ceramic materials, i.e., derived from clay, sand or cement, contain the silicon in the form of silicates. The arrangements are involving both chains of silicate ions $(SiO_4)^{2-}$, double chains and links in sheet form.
- In advance ceramic, extremely pure microscopic raw materials are used, with strict control of compositions and manufacturing conditions, in order to achieve a more uniform microstructure. Interest in modern ceramic continues to grow because these materials have a unique set of properties which no other family of materials can match. These include high hardness, heat resistance, ability to withstand corrosive atmosphere, resistance to abrasion, ability to sustain compressive loads at elevated temperatures, and an inexpensive and abundant availability of raw materials. Except for their brittleness, the ceramics stand out well against metals and plastics and can be applied as thermal barrier coatings to protect metal structures, wearing surfaces, or as integral components by themselves. These new ceramics are called either "new ceramics or fine ceramics" or frequently called "high-performance ceramics" as described by (Shinroku, 1986). Advance ceramic materials are being used in many new applications and have been proposed for numerous components which may result in significant growth of current and new business (Doremus, 1994; Lewis, 1989; Michael, B. 2007).

In advance ceramic, extremely pure microscopic raw materials are used, with strict control of compositions and manufacturing conditions, in order to achieve a more uniform microstructure. Interest in modern ceramic continues to grow because these materials have a unique set of properties which no other family of materials can match. These include high hardness, heat resistance, ability to withstand corrosive atmosphere, resistance to abrasion, ability to sustain compressive loads at elevated temperatures, and an inexpensive and abundant availability of raw materials. Except for their brittleness, the ceramics stand out well against metals and plastics and can be applied as thermal barrier coatings to protect metal structures, wearing surfaces, or as integral components by themselves. These new ceramics are called either "new ceramics or fine ceramics" or frequently called "high-performance ceramics" as described by (Shinroku, 1986). Advance ceramic materials are being used in many new applications and have been proposed for numerous components which may result in significant growth of current and new business (Doremus, 1994; Lewis, 1989; Michael, B. 2007).

1.1.1 Glass ceramics

Glass ceramic materials are fine grained polycrystalline solid containing residual glass phase formed by melting of glass and forming into products by the way of controlled crystallization of a specially formulated glass (Shackelford, & Doremus, 2008). These are primarily silicates containing oxides such as Al_2O_3, TiO_2, LiO_2, and others. In amorphous form, the glasses are transparent. Glasses can be made to transform into a polycrystalline state by a suitable heat-treatment process, called devitrification. An initiator, such as TiO_2, is added to begin the nucleation of ceramic crystals. The product is called glass ceramic. Glass ceramics are members of ceramic family and an important electroceramic type, were first investigated in the 1940s by Stookey at Corning Glass, (Pannhorst, 1995**)** are extensively exploited as electrical insulators in electronic industries and have a wide variety of

technological applications such as microelectronic substrates and packaging, optically transparent components, biomedical implants, catalytic supports, membranes and sensors, as well as for the matrix of composite materials. (Partridge, 1994; Manfredini, et al., 1997). In addition, they have been used in protection layers, sewing-thread in industry, ceramic tiles and also to develop into a very promising substrate material of computer hard disk (Novaes et al., 1994). The universal glass ceramics are Lithia-alumina-silica (Li_2O-ZrO_2-SiO_2-Al_2O_3, LZSA) systems (Montedo et al., 2009) that have zero thermal expansion co-efficient, and hence no thermal shock problem.

The majority commercial glass-ceramic products are formed by highly automated glass-forming processes and converted to a crystalline product by the proper heat treatment. Glass-ceramics can be prepared through a powder processing methods, in which glass frits are sintered and crystallized. The range of potential glass-ceramic compositions is therefore particularly wide, requiring only the ability to form a glass and control its crystallization. Glass-ceramics can provide advantages over conventional glass or ceramic materials, by combining the simplicity and flexibility of forming and inspection of glass with improved and often unique physical properties in glass ceramic. They possess highly uniform microstructures, with crystal sizes (<10mm), this homogeneity indicates that their physical properties are highly reproducible. The glass-ceramics are fully densified with zero porosity. They generally are at least 50% crystalline by volume and often are >90% crystalline (Strand, 1986). Glass-ceramics are also called as pyrocerams, vitrocerams, devitrocerams, sitalls, slag-ceramics, melt-formed ceramics, and devitrifying frits.

1.1.2 Ceramic processing and crystal growth

Glass-ceramic materials are fabricated (green body) by means of either bulk or powder processing methods. In these methods, glass-ceramic products are melted and fabricated to shape in the glass state. Most forming methods are rolling, pressing, spinning, casting, and blowing. The product is then crystallized using a heat treatment designed for that material. This process, known as ceramic processing, usually comprise of a low temperature hold to

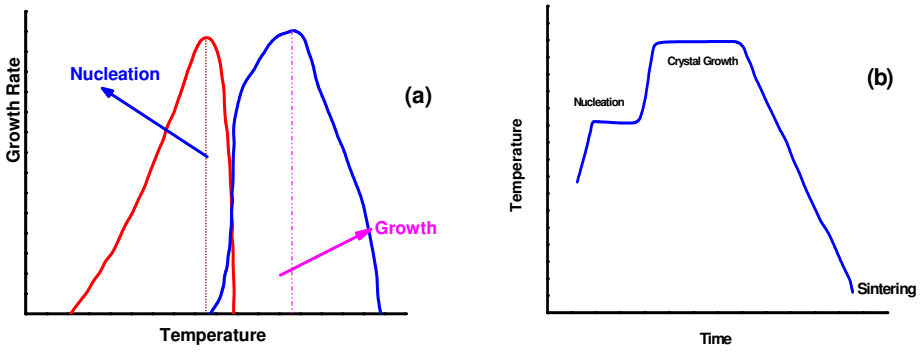

Fig. 1. (a-b): Crystal growing process (a) Nucleation and crystal growth as a function of temperature (b) heat treatment cycle showing crystal growth during sintering as a function of time.

induce nucleation, followed by one or higher temperature holds to promote crystallization and growth of the primary phase. Because crystallization occurs at high viscosity, product shapes are typically preserved with little or no shrinkage (1-3%) or deformation during the ceramming. Nucleation generally begins with phase separation, whereby an amorphous, homogeneous glass unadulterated into two immiscible phases of different compositions. Controlled devitrification is only possible for certain glass compositions and generally takes place in two stages: formation of submicroscopic nuclei, and their growth into macroscopic crystals. These two stages are called nucleation and crystal growth as shown in Figure 1(a-b) (Hölland,et al., 2002; Rincón, 1992).

Nucleation occurs when a small piece of soil forms from the liquid. The solid must achieve a certain minimum critical size before it is stable. Growth of crystal occurs as atoms from the liquid are attached to the tiny solid until no liquid remains. Devitrification means the formation of crystals on or inside of amorphous glass, typically due to a delayed cooling cycle. The presence of local crystalline inclusions supports the glass and makes it more flexible, reducing the presence and severity of micro-cracks and acting as crack stoppers. The heat treatment that supports the growth of these native crystals during the glass formation is called ceramming and it is a two step process. Ceramming is a controlled crystallization of the glass that results in the formation of tiny crystals that are uniformly distributed throughout the body of the glass structure. The size of the crystals, as well as the number and rate of growth is measured by the time and temperature of the ceramming heat treatment. There are two branch of ceramming process; crystal nucleation and crystal growth as shown in Fig. 2(a-c) **(**Steffestun, & Frischat, G.H. 1993; Durrani et al., 2005; Cattell, M.J. 2006). Each phase take place because the glass body is detained at exact temperature for a definite length of time. Crystals have a propensity to develop in a mixture of glass when it is held at a specific temperature, called the crystal nucleation temperature. This means that when apprehended at the crystal nucleation temperature, multiple seed crystals begin to grow throughout the glass body. The longer the glass is kept at this temperature, the more seed crystals will form. Ideally, a glass ceramic will be strongest when there is a very large number of a small crystal distributed uniformly all over its mass. Once a seed crystal forms, it will also begin to grow larger at this temperature, but somewhat slowly. If the temperature of the glass body is held at the crystal nucleation temperature for a very long time, a very large number of crystals of broadly varying size will form. The initially the seed will be largest, while the crystals that have lately begun to grow, will be the smallest. In order to better control the art of the finished product, the ideal glass ceramic will have crystals of a small and uniform size. Any form of devitrification in a glass structure will produce one degree of opacity. Large crystals are flat to make the glass opaque, while small crystals uniformly scattered throughout the structure have less of an impact on the optical qualities of the finished product. Thus it is of advantage to keep the temperature at the point of maximum seeding for a finite length of time in order to allow several tiny seed crystals to nucleate, and then to stop the nucleation process and support the ones that have formed to grow to appropriate size.

The glass ceramic materials with tailor made properties can be fabricated by controlling nucleation and crystal growth process. Although some glass compositions are self-nucleating, generally some nucleating agents are added to the batch to promote phase separation and internal nucleation. These melt homogeneously into the glass, but promote

very fine phase separation on reheating. The isolated phase, which can be a metal, titanate, zirconate, phosphate, sulfide, or halide, is structurally incompatible with the host glass and is usually highly unstable as a glass. Nucleation is followed by one or higher temperature treatments to promote crystallization and development of the desired microstructure. Most commercial glass-ceramic products are formed by highly mechanized glass-forming processes and converted to a crystalline product by proper heat treatment. Glass-ceramic materials have been prepared through powder processing in which glass frits are sintered and then crystallized (Grossman, 1974) the range of potential glass-ceramic compositions is therefore extremely broad, requiring only the ability to form a glass and control its crystallization. The production of glass-ceramics from powdered, using conventional ceramic processes such as spraying, slip-casting, or extrusion, extends the range of possible glass-ceramic compositions by taking advantage of surface crystallization. In these materials, the surfaces of the glass grains serve as the nucleating sites for the crystal phases. The glass composition and processing conditions are selected such that the glass softens proceeding to crystallization and undergoes viscous sintering to full density just before the crystallization process is completed. Given these conditions, the final crystalline microstructure is basically the same as that produced from the bulk process.

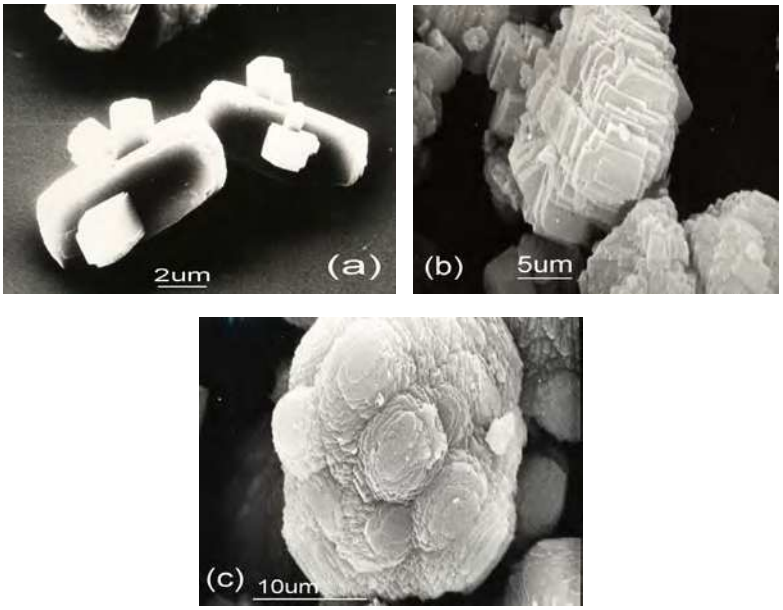

Fig. 2. (a-c): Crystal growing in aluminosilicate ceramic materials (a) Aluminum deficient silicalite-I (b) High silica aluminosilicate (c) sodium aluminosilicate.

The precursor glass powders may be produced by various methods, the simplest being the milling of quenched glass to an average particle size of 3-15mm. Sol-gel processes (Yuan, et al., 2010; Chen, et al., 2010; and Lei, B. 2010) in which highly uniform, ultrafine amorphous particles are grown in a chemical solution, may be preferable for certain applications. Such devitrifying frits are employed significantly as sealing frits for bonding glasses, ceramics,

and metals. Other applications include co-fired multilayer substrates for electronic packaging, matrices for fiber-reinforced composite materials, refractory cements and corrosion-resistant coatings.

1.1.3 Machinable glass ceramic

Machinable glass ceramics based on magnesium aluminum silicate ($MgO\text{-}Al_2O_3\text{-}SiO_2$, MAS) glass ceramic system have technological importance due to their applications for high voltage and in ultra high vacuum (Hattori, T. et al., 1982, Emad M El-Meliegy, 2004). An important group of these materials are mica-containing glass-ceramics. The crystal phase generated in the mica containing glass ceramics is called fluorophlogopite ($KMg_3AlSi_3O_{10}F_2$) receive wide application due to their high machinability, which results in an increased versatility of the products and numerous possibilities for industrial application.These materials not only have strange feature of machinability but also have potential use till date are in electronic and semiconductor industry (precision coil formers & high voltage insulators), laser industry (spacers, cavities and reflectors in laser assemblies), high vacuum industry (thermal breaks in high temperature processing equipment, coil supports), aerospace and space Industry (retaining rings on hinges, windows and doors of NASA's space shuttle, supports and components in several satellite borne systems) and also in nuclear industry (fixtures and reference blocks in power generation units). It is noted (Hench et al., 1993) that glass ceramics can also be used for biomedical purpose including dental materials field. The MAS glass ceramic can be machined into complicated shapes and precision parts with ordinary metal working tools, quickly and inexpensively, and it requires no post firing after machining, no frustrating delays, no expensive hardware, no post fabrication shrinkage, and also no costly diamond tools to meet the required specifications. MAS ceramic material exhibits non-wetting, zero porosity, withstands high temperatures up to 1000^{o}C and has high dielectric strength. MAS materials are being used in nuclear technology (Bozadzhiev L.S.; 2011) in the production of proto type components, used in medicines for the axles of mechanisms providing energy for implanted cardio-stimulators and also used in the production of welding jets or as holders for welded components. MAS have potential application in spacers, headers and windows for microwave tube devices, sample holders for microscopes and aerospace components (Goswami et al., 2002; Baik, et al. 1995; Boccaccini, 1997). Properties of MAS glass ceramics such as hardness, machinability, conductivity depend upon the composition and microstructure. Machining of these materials can be carried out to precise tolerances and surface finish with conventional tools. Factual reason of good machinability character of MAS lies in unique microstructure of inter-locking array of plate like mica crystals, dispersed uniformly throughout glass matrix.

MAS glass ceramic materials have been prepared by controlled crystallization in which a large number of tiny crystals rather than few bigger single crystals have been grown (Margha, et al., 2009). Controlled crystallization or heat treatments generally consist of a two-stage heat treatment, namely a nucleation stage and crystal growth stage. In the nucleation stage, small nuclei are formed within the parent glass. After the formation of stable nuclei, crystallization taking place by growth of a new crystalline phase. The nucleation and crystallization parameters of glasses are very significant in the preparation of glass-ceramics with desired microstructures and properties (Abo-Mosallam, 2009).

Simmons, et al, 1982; studied the effect of fluorine content and its source on the crystallization of MAS materials. Identified predominant crystalline phases in their study were fluorite, norbergite or fluorophlogopite depending on heat treatment, fluorine concentration etc. Common preparation methods have been discussed in literature (Hattori, T. et al. 1982) but due to special category and technological importance of the material, the crucial process has either been vague or missing. Recently, magnesium aluminum silicate (MAS) glass ceramic systems have been synthesized by sintering route (Durrani, et al., 2010 & Hussain, S.Z et al., 2010). Therefore, the preparation of MAS materials acquires special importance for meeting indigenous requirement. In the light of this fact, preparation of machinable MAS glass ceramic was undertaken using sintering route.

1.2 Sintering

Generally, when ceramic powders are formed and then heated (green compact) part, there is a certain temperature below melting point at which they begin to burn, and in most cases there is shrinkage or expansion resulting in densification, phenomenon is called sintering. (Moulson et al. 1992; Rahaman, 2005). The goal of the sintering process is to convert highly porous compacted powder into high strength bodies. Sintering may be considered the process by which an assembly of particles, compacted under pressure or simply confined in a container, chemically bond themselves into a coherent body under the influence of an elevated temperature. The temperature is usually below the melting point of the major constituent. Much of the difficulty in defining and analyzing sintering is based on the many changes within the material that may take place simultaneously or consecutively. In the sintering process the temperature of the granulated sinter compound is raised to temperatures between 1000^{o}C and 1450^{o}C to achieve partial fusion. During the heating and cooling cycle different species react with each other to produce certain phases. Molten material is produced which crystallizes or solidifies into various phases that bond the microstructure together. Therefore, sinter consists of an assembly of various phases of varying chemical composition and morphology. Each of different phases has a unique influence on the sinter quality.

Sintering is a complex process and for any given metal and set of sintering conditions there are likely to be different stages, driving forces and material transport mechanisms associated with the process. Sintering or firing of pure oxide ceramic requires relatively long time and high temperature because the diffusion proceeds in solid state. The complete sintering process is generally considered to occur in three stages: (i) initial stage, (ii) intermediate stage, (iii) and final stage. There is no clear-cut distinction between the stages since the processes that are associated with each stage tend to overlap each other.

The reduction in surface energy can be used to explain the three main stages of solid-state sintering, (Wang, Y., 2008) is shown in Fig. 3(a-c). In the first stage, atoms migrate towards the points of contact between particles to form necks as this filling process reduces the surface area and the surface energy. In the second stage, the grain boundaries grow because, as atoms are removed from the grain boundary and diffuses towards the neck, this causes the centers of particles to mutually converge. In the final stage, the grain is slowly eliminated as grain boundaries merge.

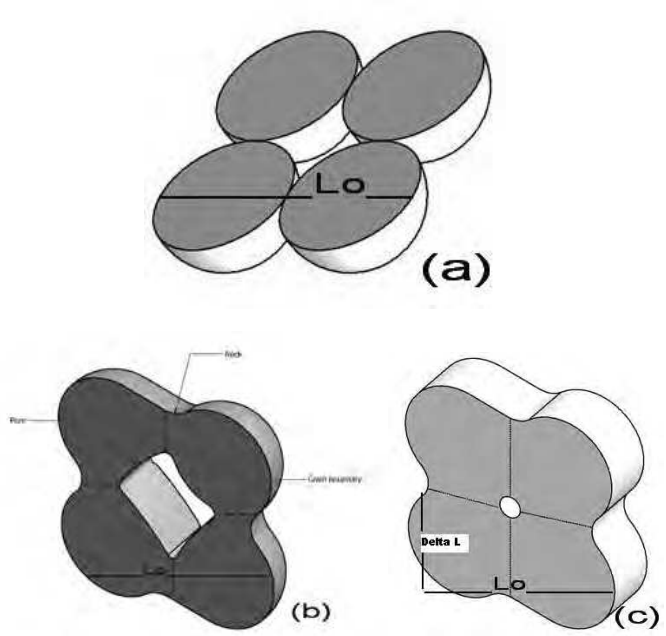

Fig. 3. (a-c): Schematic representation of the neck formation during solid-sintering due to (a) powder compaction, (b) neck growth, and (c) neck growth developed by densification.

The description of such topic is beyond the scope of this chapter, however, a detailed account of these stages has been discussed somewhere else (Richerson, 1992; & German, 1996). The sintering process is an important tool in fabrication of various materials into useful products. Today, it is used to manufacture a wide range of products for consumers, electronics, transportation and biomedical systems, e.g., rocket nozzles, ultrasonic transducers, automobile engines, semiconductor packaging substrate, and dental implants. Sintering is not only used for high temperature materials but also for other materials that can be densified below 1000°C. For example, firing of glass-based substrate and of-screen-printed metallic inks or paste for microelectronic applications. Densification or shrinkage of the sintered part is very often associated with all types of sintering. However, sintering can take place without any shrinkage; expansion or no net dimensional change is quite possible. From the tooling point of view it is preferred to avoid very large amount of dimensional changes. The driving force for solid state sintering is the excess surface free energy. Sintering converts a compacted powder into a denser structure of crystallites joined to one another by grain boundaries. Grain boundaries vary in thickness from 100pm to over 1µm.They may consist of crystalline or vitreous second phases, or may be simply a disordered form of the major phase because of differing lattice orientation in the neighboring grains. Grain boundary is the border between two grains, or crystallites, in a polycrystalline material. Grain boundaries are generally not as dense as the crystals and, in the early stages of sintering at least, allow free diffusion of gas to and from the outside atmosphere. Typically, polycrystalline ceramic's microstructure is developed by solid state sintering as shown in Fig. 4(a-c).

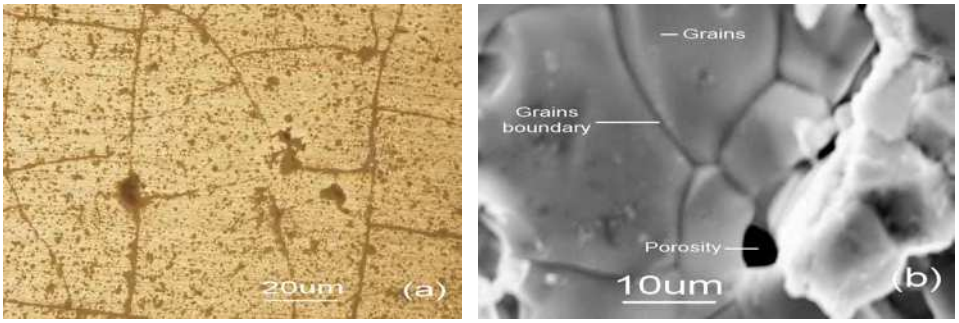

Fig. 4. (a-b): Microstructure of sintered pellet of (a) Metallographic image of magnesium aluminum silicate glass ceramic (MAS-G4) (b) SEM image showing combinations of grains, grain boundaries and porosity.

The polycrystalline ceramic's microstructure consists of numerous grains or crystallites that are defined by the long-range order of the crystal. These grains are separated by a grain boundary that may include single or multiple phases of sintered aid material. A grain boundary is the surface that separates the individual grains and is a narrow zone in which the atoms are not properly spaced. In addition, microstructure is likely to contain a certain amount of porosity left behind during manufacture. Sometime separate phases of material exist within the microstructure as particles as is commonly found in reaction-bonded ceramics (Swab, 2009). During the sintering process, an agent (sintering aid) is added to help in the bonding process and reduced the temperature that is required during the sintering step. These sintering agents lead to a reduction in the mechanical properties of ceramic because they form relatively soft grain boundaries with low melting temperatures. Smaller particles sinter much faster than coarse particles because the surface area is larger and the diffusion distances are smaller. Rate of sintering varies with temperature. Sintering processes can be divided into three large categories (Yu, et al., 2001; Moghadam, et al.1982):

i. Solid Phase Sintering
ii. Liquid Phase Sintering
iii. Gas Phase Sintering

1.2.1 Factors effect the sintering

The most important factors involved during sintering process are "process variables" (temperature, time and furnace atmosphere), "materials variables" (particle size, shape and structure), green density and dimensional changes. Variety of sintering methods are available for sintering the ceramic compacts i.e., standard pressure sintering, reaction-sintering, hot pressing, post-reaction sintering, recrystallization sintering, atmospheric pressure sintering, ultra-high-pressure sintering (Ring, T.A. 1996), chemical vapor deposition (CVD) (Mitchell, (2004) and isostatic hot pressing (HIP) (Olevsky, et al. 2009, Smothers, 2009).

1.3 Aim of work

The present work concerns only about solid phase sintering process. It is very difficult to sinter fully dense state of machinable magnesium aluminum silicate (MAS) glass ceramic

materials with fluorophlogopite as the main crystalline phase. The primary objective of the present research work is to provide a simple sintering method for preparation of crystalline magnesium aluminum silicate glass-ceramic body with predominant fluorophlogopite crystal phase, which can be utilized as candidate material for machinable tools acquiring good resistance to attack by acids and alkalies. The variation in sintered densities, mechanism of phase transformation, microstructure changes and thermal expansion co-efficient of MAS glass ceramic was also ascertained. It constitutes a part of our ongoing studies on MAS glass ceramic material in detail and all the results are based on techniques previously applied (Durrani et al., 2010; Hussain et al. 2010).

2. Preparation of MAS glass ceramic by sintering route

Magnesium aluminum silicate glass ceramic specimens (designated as MAS-G1-MAS-G10) were prepared through sintering route using three stage schedules i.e. calcination, nucleation and crystallization process using stiochiometeric amount of inorganic metal salts, such as oxides, hydroxide, fluorides and carbonates in weight percent as shown in **Table 1**. The starting raw materials used in the present study were Silica (SiO_2, Fluka, 99.9%), aluminum oxide (Al_2O_3, BDH, 99.9%), magnesium oxide (MgO, Merck, 99.9%), potassium carbonate (K_2CO_3, Riedel-de Haen 99.9%), boron oxide (B_2O_3, BDH, 99.9%), magnesium fluoride (MgF_2 BDH99.9%), ortho-phosphoric acid (H_3PO_4.BDH, 99.9%), acetone (CH_3COCH_3 BDH, 99.9%), hydrochloric acid (HCl, Marck), sodium carbonate (Na_2CO_3, BDH, 99.9%) and sodium hydroxide pellets (NaOH, Merck). All chemicals were of analytical reagent grade and used without further purification.

In a typical preparation, the initial charge was mixed thoroughly and calcined at 950^0C for 24 h with a pre-determined heating schedule. Approximately 4-7wt% MgF_2 was added to calcined charge and milled in a planetary ball mill for 40 h. The median particle size of the ball-milled sample was around 5.3μm. The fine ball milled charge was seasoned in 5% H_3PO_4 acid solution in acetone medium for 72h. Compacts of MAS (61×16×5 mm) were made using hydraulic press of load capacity ~ 25 tons/in^2 (1 ton/in^2 = 15.44 MPa). The compacts were sintered using two-step heating program. In first step the compact was heated up to 600-630^{o}C for 2-4 h to ensure good nucleation and to initiate crystal growth. In second step, heating was carried out with different heating rates in the range of 15-60^{o}C/h up to sintering temperatures of 950-1080^{o}C. The sample was kept at the sintering temperature for a sufficiently long time to achieve the desired crystal growth. In order to measure the phase purity, crystallinity and morphology of synthesized products, the MAS materials were characterized using different analytical techniques i.e., TG/DTA, XRD/XRF and SEM. Phase purity and crystallinity of MAS specimens was determined by X-ray diffraction on a Rigaku Geiger flux instrument using Cu Kα radiation. For measurement of weight loss the combined TG-DTA thermal analysis was performed using Netzsch STA-409 thermoanalyzer. Coefficient of thermal expansion was observed on horizontal high temperature computer-controlled differential dilatometer (Netzsch, DIL, 409) with heating rate of 10°C/min up to 1100°C in static air. The particle size distribution of powder specimens was measured by laser particle size analyzer (SK-Laser Micron PRO-7000S). Density of MAS specimens was measured using Ultra Pycnometer 1000 (Quantachrome). Porosity was measured by radiographic technique using Real-time radiography Instrument (Model Isvolt HS Panta Sei Fert). Micro-structural features, elemental contents and porosity

of sintered specimen MAS -G8 were observed using scanning electron microscope (SEM, LEO 4401). The specimen was fully polished, put onto aluminum stud, dried in air and then the specimen was coated with thin gold film for the SEM observation. For the measurement of micro-hardness of sintered specimens, indentation technique using Vickers diamond pyramid indentor on the micro hardness tester was used. Before measurements, the sample surface was polished with 3μ alumina powder to get good reflective surface. The measurement was done on the polished surface by applying 300g load for 15 sec. The effect of K_2CO_3 concentration on sintered density and mechinability of MAS specimens (MAS-K1-MAS-K10) at fixed amount of MgF_2 (4-11%) and nucleation temperature (630^{o}C) was also studied. The sintered specimens were treated with 5% hydrofluoric and hydrochloric acids for 24h at 95^{o}C to observed the effect of these acids. Effect of 5% sodium hydroxide and sodium carbonate was also studied for 6 h duration at 95^{o}C. The samples were weighed for any loss in weight after washing off acids and bases.

Impedance spectroscopy on pellets of MAS glass ceramic, which were sintered at 1040 and 1050^{o}C temperatures was performed in the frequency range of 1 ≤ frequency ≤ 10^7 Hz at room temperature, using an alpha-N Analyzer (Novocontrol Germany). The surfaces of both sides of the pellets were cleaned properly and contacts were made by silver paint on opposite sides of the pellet, which were cured at 150^{o}C (423K) for 3 h. Before the impedance experiments, the dispersive behavior of the leads were carefully checked to exclude any extraneous inductive and capacitive coupling in the experimental frequency range. The ac signal amplitude used for all these studies was 0.2 V and WINDETA software was used for data acquisition.

Specimen #	Chemical Composition (wt %)						Calcination		Ball Milling	Soaking
	SiO_2	Al_2O_3	MgO	K_2CO_3	B_2O_3	MgF_2	Temperature (^{o}C)	Time (h)	Time (h)	
MAS -G1	36.62	12.73	16.87	13.93	1.91	17.91	950	24	40	72
MAS -G2	37.57	13.19	16.49	14.26	1.97	16.49	950	24	40	72
MAS -G3	37.72	13.23	16.05	13.98	2.48	16.54	950	24	40	72
MAS -G4	38.51	13.51	16.38	14.27	2.53	14.78	950	24	40	72
MAS -G5	39.28	15.71	15.52	13.59	8.25	7.65	950	24	40	72
MAS -G7	40.67	16.43	14.12	13.43	8.62	6.73	950	24	40	72
MAS -G8	36.34	24.82	13.23	11.32	3.53	10.76	950	24	40	72
MAS -G9	44.32	12.91	15.45	13.62	4.12	9.58	950	24	40	72
MAS -G10	41.75	14.15	16.92	13.54	4.46	9.18	950	24	40	72

MAS-G = Magnesium aluminum silicate glass

Table 1. Chemical composition and reaction conditions for preparation of MAS glass ceramic material by sintering route.

3. Results and discussion

3.1 XRD phase analysis

Experimental results showed the phase stability, thermal stability, compressibility, and sinterability of MAS glass ceramic materials. The crystallinity of MAS glass was studied by

XRD and XRF. The XRD patterns of specimens MAS-G3, MAS-G4 and MAS-G8 sintered at 1040°C for 3h along with standard specimens are presented in Fig. 5. The XRD patterns were indexed and compared with Joint Committee of Powder Diffraction Standard (JCPDS) data cards (McClune, W. F.1989). The predominant phases in the prepared MAS specimens were identified as fluorophlogopite (potassium magnesium aluminum silicate, $KMg_3AlSi_3O_{10}F_2$, JPCPD # 71-1542), sillimanite (aluminum silicon oxide, Al_2SiO_5, JPCPD #.88-0893) and leucite (potassium aluminum silicate $KAlSi_2O_6$ JPCPD # 15-0047). The percentage of these phases in each specimen is given in **Table 2,** whereas crystallographic XRD analysis data are presented in **Table 3.** The well formed diffraction patterns and "d" values confirmed that the predominant crystal phase in MAS-G8 is 57% fluorophlogopite and this fluorophlogopite crystal phase was found near to standard values i.e., 60% fluorophlogopite. It was also observed that specimen MAS-G8 consists of 57%fluorophlogopite crystal phase due to which it possess very good mechinability, but very difficult to be sintered to fully dense state. The leucite (potassium-aluminum-silicate, $KAlSi_2O_6$) crystal phase with large coefficient of thermal expansion is formed when glass ceramic is heated and held at temperatures between 1025°C and 1530°C.

Specimen #	Sintering Conditions			Density (g/cm^3)		Phase (%) by XRD	
	Nucleation (^{o}C)	Temperature (^{o}C)	Time (h)	Green	Sintered		
MAS-G1	630	1040	3	1.79	2.18	F= 28	L= 71
MAS-G2	630	1040	3	1.74	2.12	F= 30	L = 69
MAS-G3	630	1040	3	1.91	2.29	F=51	S= 49
MAS-G4	630	1050	3	1.68	2.15	F = 56	S = 43
MAS-G5	630	1040	3	1.65	2.12	F= 28	L= 71
MAS-G6	630	1050	3	1.72	2.14	F=49	S= 42
MAS-G7	630	1060	4	1.64	2.14	F = 50	S = 44
MAS-G8	630	1040	3	1.81	2.38	F= 57	S = 43
MAS-G9	630	1070	2	1.86	2.39	F= 54	S = 42
MAS-G10	630	1080	2	1.74	2.35	F= 51	S = 39
Standard					2.48	F= 60	S = 40

F= Fluorophlogopite L= Leucite and S= Sillimanite

Table 2. Fluorophlogopite phase of magnesium aluminum silicate glass ceramics with different composition.

Crystallographic XRD analysis	Fluorophlogopite	Silliminite
Symmetry	Monoclinic	Orthorhombic
Unit cell volume(Å^3)	481.77	331.23
Crystallite size (Å)	184	184
Lattice parameters		
a (Å)	5.308	7.49
b (Å)	9.183	7.67
c (Å)	10.00	5.77

Table 3. XRD phase analysis of MAS-G8 specimen.

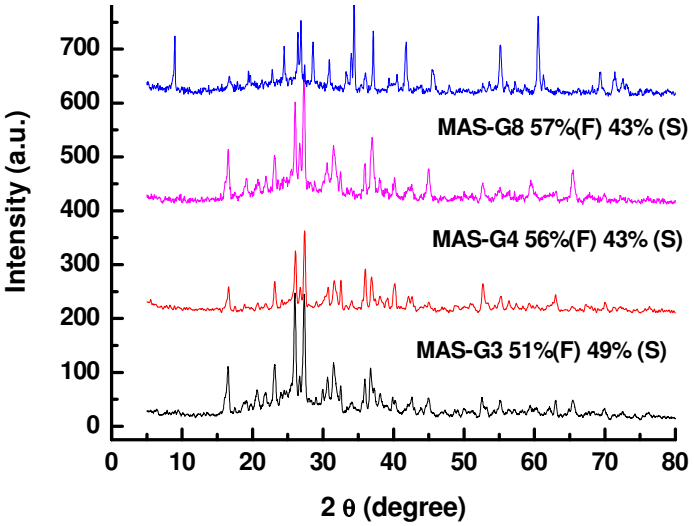

Fig. 5. XRD patterns of magnesium aluminum silicate glass ceramic, specimen MAS-G3, MAS-G4 and MAS-G8 along with standard.

3.2 Thermal analysis

The TG/DTA analysis is proper method to determine the optimal stabilization temperature (Perdomol, et al., 1998; & Izquierdo-Barba, et al., 1999). Thermal analysis TG, DTA of selected specimen the MAS-G8 was carried in the temperature range of 40-1000°C in order to find the crystallization temperature of different crystalline phases as shown in Fig. 6. The total weight loss 9.14% was observed after heating up to 900°C. Since the specimen was not fully dried, some physically bounded water was present at surface of crystals and in micropores, which caused a subsequent loss of mass at the lowest temperature range, i.e., 50-250°C. This process is endothermic as confirmed by DTA. Two peaks in the DTA data were observed. The first peak is endothermic, which is connected with decomposition of water vapors and glass transformation. It can be seen that crystal phase (nucleation) occurs at nearly 732°C, which is evident from the large exothermic peak. The exothermal maxima correspond to the separation of the crystalline phase. The position of the minimum on DTA curve is basically determined by the chemical composition of the separated phase or by its transformation temperature. The exothermal crystallization peak, its position and shape have been characterized by the crystallization process (Bapna & Mueller, H. 1996). In crystallization process [K_2O-Al_2O_3-SiO_2-MgO-B_2O_3-F], first crystal phase to appear is the aluminium borate-mullite solid solution crystal which on increasing temperature, transforms to fluorophlogopite on reaction with the matrix phase (Roy, S. et al. (2011). Heating rate during DTA is around 10°C/min. All the volatiles were completely removed at 900°C. The nucleation temperature of this crystal is a strong function of heating rate as found by (Bapna & Mueller, H. 1996) and observed that with increasing heating rate shifts the nucleation temperature to a higher value. The percent weight loss of other specimens MAS-G2 to MAS-10 is shown in Table 4.

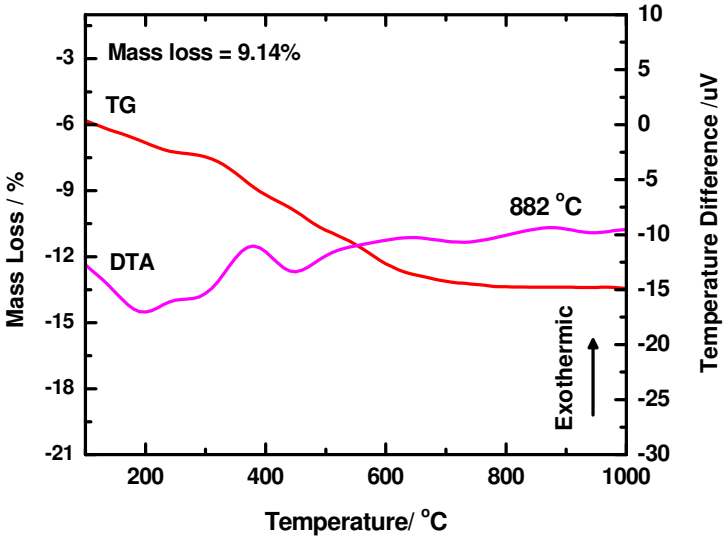

Fig. 6. TG/DTA curves for magnesium aluminum silicate glass ceramic powder, specimen MAS-G8.

3.3 Green compact and thermo dilatometric study

The behavior of densification was measured by dilatometry in order to understand what is occurring during sintering. Dilatometry is a well-known method of studying densification kinetics during the sintering process of ceramic bodies (Holkova, *et al.,* 2003). In dilatometry, the compacted ceramic body undergoes heat treatment in the dilatometer to initiate sintering. Simultaneously, the length of the compacted body is measured as a function of time at a given temperature. The densification can further be assessed by measurement of post-sintering density, whereby as the compacted body shrinks, its density will increase. Isothermal sintering experiments were carried out by heating samples rapidly after binder burnout to the sintering temperature and the data collected at intervals that are set in the control program. An entire densification profile can be obtained from a single sample. The characteristics of pressed powder of MAS-G4 and MAS-G8 during sintering were examined by means of dilatometry. Fig. 7 and Fig.8 display the thermo-dilatometric curves of MAS-G4 and MAS-G8 powders which were calcined at 650°C and then pressed into green pellet respectively. The curve shows a simple thermal shirking or expansion i.e., the change in length during sintering of pellet. There was no change in length on heating up to temperature of 208°C but started at about 557°C. However, a large shrinkage occurred as a result of evolution of decomposed species between 300 and 400°C. The temperature between 400 and 700°C shows the expansion in the material. This expansion is due to nucleation process i.e. decomposition of meat-stable phases of magnesium and aluminum silicates and carbonates and fluorides also the expulsion of organic binder (PVA). Above 850°C, there is gradual increase in dimensional changes (lattice parameters) which are due to crystal growth (development of MAS-G8 crystalline phase). On the basis of dilatometry results, sintering was conducted between 985-1040°C in order to obtain the crystalline MAS-G8

fluorophlogopite phase. Thermal expansion co-efficient (alpha) of MAS-G8 ceramic was measured at different temperature ranges by dilatometric technique. The coefficient of thermal expansion (α = x10^{-5} ^{o}C^{-1}) was measured using a dilatometer Fig. 7(a-b) and Fig. 8(a-b) in air at 1000^{o}C for specimens MAS-4 and MAS-G8; the values are -1.563 and -1.093 x10^{-5} ^{o}C^{-1} respectively. The result revealed that α decrease with increase of chemical composition. The detailed coefficient of thermal expansion (α = x10^{-5} ^{o}C^{-1}) values are presented in **Table 4.**

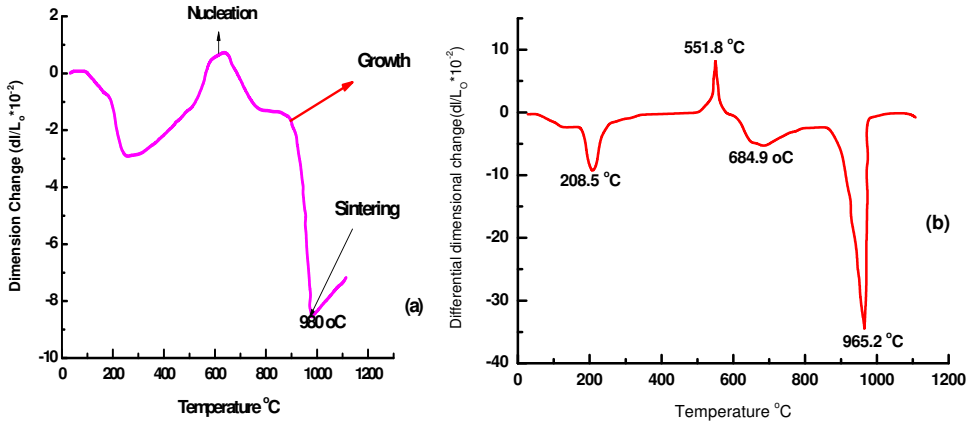

Fig. 7. (a-b): Thermodilatometric (a) and differential dilatometric (b) curves of green compact of magnesium aluminum silicate glass ceramic specimen MAS-G4.

Physico-chemical Properties						
Property	Units	MAS-G2	MAS-G4	MAS-G6	MAS-G8	MAS-G10
Weight loss (DG/DTA)	%	10.15	10.42	9.05	9.14	9.32
Thermal co-efficient (200-1100 ^{o}C)	^{o}C^{-1}	-1.563x10^{-5}	-1.563x10^{-5}	-1.563x10^{-5}	-1.093x10^{-5}	-1.063x10^{-5}
Median diameter of particle	µm	4.4	5.4	5.6	5.3	4.9
Micro hardness	Vicker	449	484	504	527	505
Resistivity	Ω	1.07 x 10^{9}	1.27 x 10^{9}	1.35 x 10^{9}	2.72 x 10^{9}	2.05 x 10^{9}
Porosity	%	7-8	7	5	2-3	2-3
Theoretical density	%	79	87	81	93	91

Table 4. Physical properties of MAS glass ceramics.

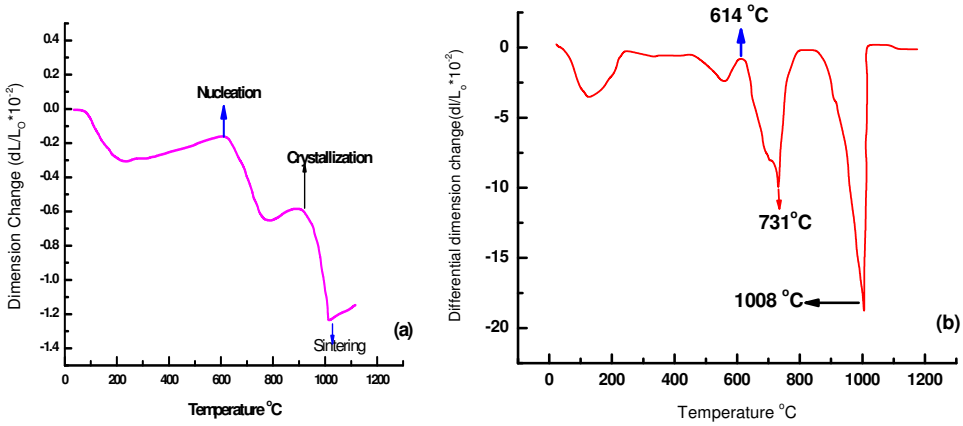

Fig. 8. (a-b): Thermodilatometric (a) and differential dilatometric (b) curves of green compact of magnesium aluminum silicate glass ceramic specimen MAS-G8.

3.4 Sintering MAS glass ceramic

Green solid briquette of dimensions (61x16x5mm) was obtained using hydraulic press. The green body exhibits significant changes of its properties resulting from dehydration at low temperatures, phase changes during dehydroxlation, high-temperature reactions, and densification during sintering. All these changes significantly influence phyisco-mechanical properties of the fired body.It was observed that if the initial charge was not pulverized for sufficiently long time after calcination, the sintered briquette had a lot of open pores on the surface and MAS glass ceramic material looks swelled and deformed as shown in Fig. 9(a-c). The percent relative densities were measured in order to evaluate the material performance. The effect of heating temperature and time duration on density of sintered specimens MAS-G6 to MAS-G10 as a function of sintering temperature is shown in **Table 2**. Insignificant increase in density was observed in sintering temperature range 1040^{o}C to 1060^{o}C with time duration range 2-4h. It was observed that as the sintering temperature was increased beyond 1060^{o}C, excessive thermal energy leads to some rearrangement among the grains as well as some an isotropic crystal growth. In addition, decomposition of fluorophlogopite phase, formed at lower temperature, takes place leading to the development of internal line cracks/voids (Radojic, & Nikolic, 1991) in the material. As a result of this, the material looks swelled, broken, deformed and its density decreases at higher sintering temperatures, Fig. 9(a-c). The important sintering parameters, green and sintered densities of samples MAS-G1 to MAS-G10 are given in **Table 2.** Relative density (93%) was obtained, when the MAS-8 glass ceramic specimen was sintered at 1040^{o}C for 4h. The high sintered density can be attributed due to small degree of agglomeration and fine nature of powder. The results revealed that sintered MAS-G8 glass ceramic is composed of uniformly sized grains and is >93% of theoretical density. Formation of fluorophlogopite phase, good relative density and micro porosity are mainly responsible for producing machinability properties. Fig.10 (a-b) shows photographic, microscopic and scanning electron image of green and sintered MAS-G4 glass specimens whereas XRD pattern of such specimen is shown in Fig. 5.

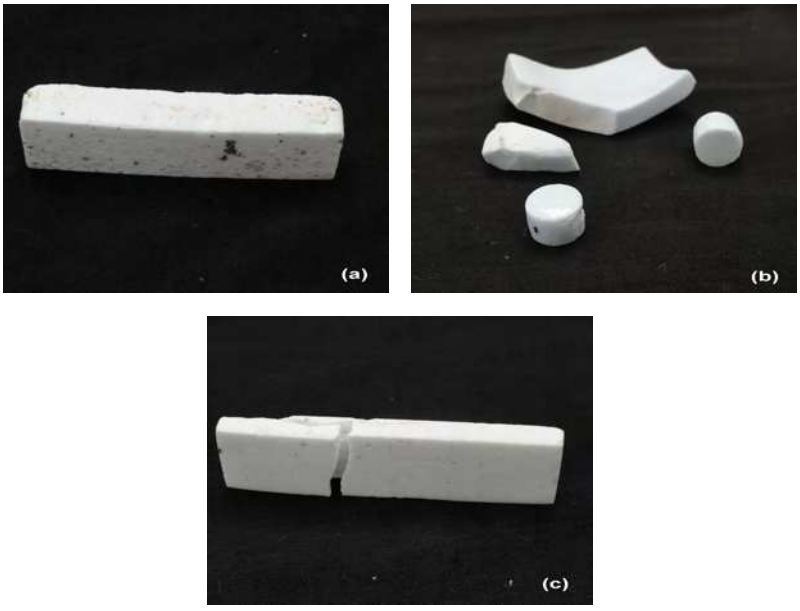

Fig. 9. (a-c): The effect of heating temperature and time duration on physical surface of sintered specimens (a) Open pores on the surface of MAS-G4 (b) Swelling of MAS material (c) brittle and broken of sintered slab.

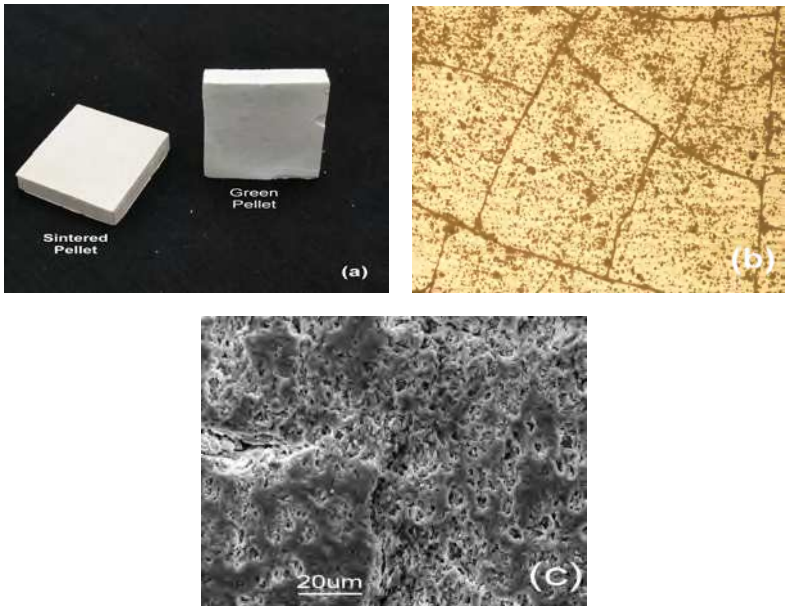

Fig. 10. (a-c): Photograph of MAS-G4 glass specimen (a) green and sintered specimens (b) microscopic image and (c) SEM micrograph of polished sintered MAS-G4 glass specimen.

3.5 Particle size distribution

The particle size distribution curve of specimen MAS-G8 powder is shown in Fig. 11. This curve revealed that the particle size distribution is < 10µm with median particle size is around 5.3µm. Smaller particle size and particle size distribution in narrow range is essential for good sinterability. Experimental results proved the same. It is also found that specimen MAS-G8 sintered at temperature 1040°C provided the material of smaller and uniform particle distribution and density ~2.35 g/cm^3 (93% of theoretical density) having 3-4% through porosity. Because of larger surface area of fine powder, the progress of sintering process accelerates even at low temperatures. However, fine particles, higher the tendency to form agglomerates retarding densification significantly (Ting, & R. Y. Lin, 1995). During pressing, it was observed that if the initial charge was not pulverized for sufficiently long time after calcination, the sintered briquette had a lot of open pores on the surface. So, in order to minimize the porosity in the sintered product, quite long period was used for pulverization and finally 72 h time duration was selected.

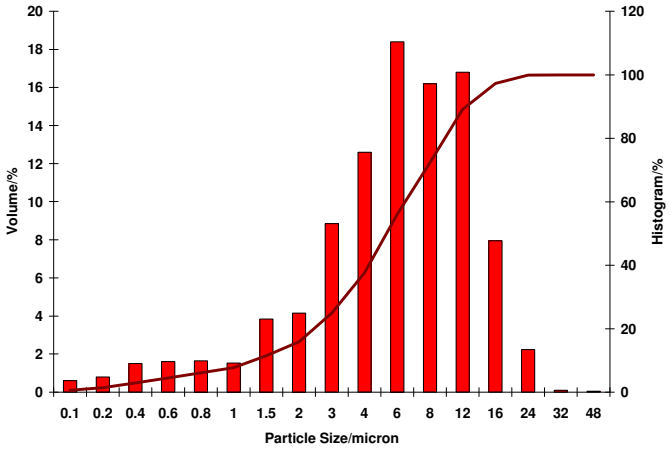

Fig. 11. Particle size distribution of magnesium aluminum silicate glass ceramic MAS-G8 powder.

3.6 Porosity

Porosity or void fraction is a measure of void spaces in a material, and is the ratio of the volume of all the pores in a material to the total volume. Radiography of specimen MAS-G4 and MAS-G8 was conducted in order to observe the porosity. Fig. 12 and Fig.13 show radiographic studies for the estimation of porosity. Porosity is the result of gas entrapment in the solidifying glass ceramic materials. Porosity can take many shapes on a radiograph but often appears as dark round or irregular spots or specks appearing singularly, in clusters, or in rows. Radiographic images as indicated in Fig. 12b and Fig.13b do not show any dark round or irregular spots or specks and do not predict any sign of porosity. It means that the specimens MAS-G8 and MAS-G4 have through porosity. However, some surface porosity was observed by SEM in both specimens MAS-G8 and MAS-G4 as shown in Fig. 14(a-b).

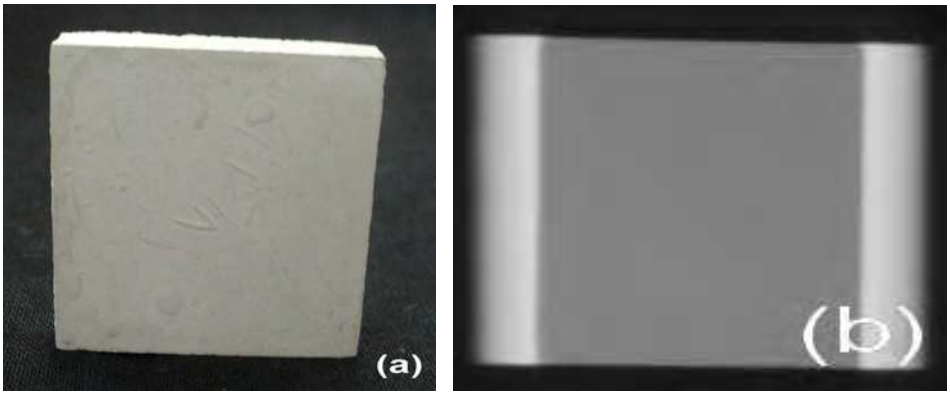

Fig. 12. (a-b): Radiographic studies of sintered specimens of magnesium aluminum silicate glass ceramic: (a) sintered MAS-G4 (b) Radiographic image of MAS-G4.

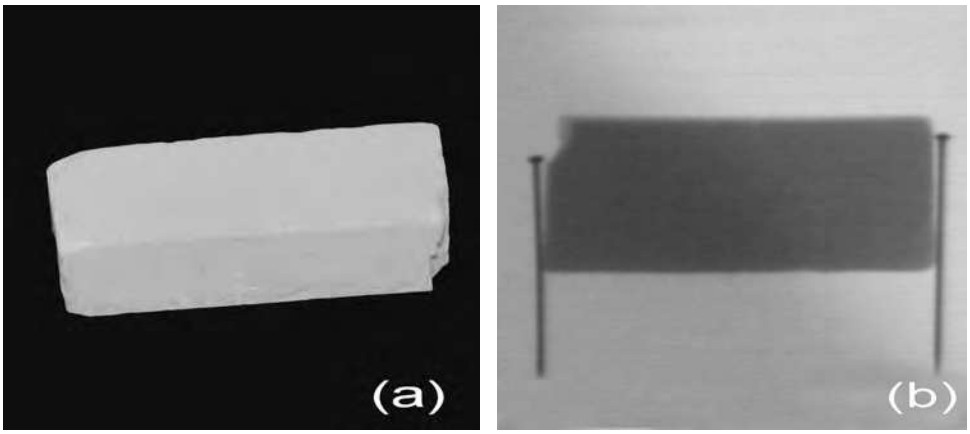

Fig. 13. (a-b): Radiographic studies of sintered specimen of magnesium aluminum silicate glass ceramic (a) sintered MAS-G8) (b) Radiographic image of MAS-G8.

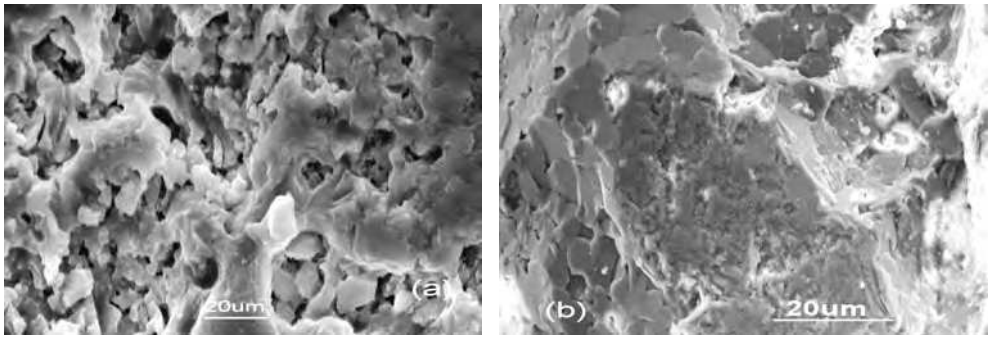

Fig. 14. (a-b): SEM image of magnesium aluminum silicate glass ceramic (a) MAS-G8 and (b) MAS-G4.

3.7 Resistance measurement

The impedance plane plots of MAS glass specimens sintered at 1040 and 1050°C at room temperature are shown in Fig.15 and Fig.16. The Fig.15b and Fig.16b show the typical impedance plane plots between real (Z/) and imaginary parts (Z//) of impedance. An arc-like behavior was noticed in both the plots and the intersection of the arc at low frequency (right hand side) gives the total resistance of the specimens , whereas, intersection at high frequency (the extension of arc on the left hand side) passes through origin. When MAS-G4 glass specimen heated to 1050°C, the intersection of arc on the right hand side shows a decrease in the magnitude of Z/, when sintering temperature is increased from 1040°C to 1450°C. This decrease can be explained as heating will cause grain growth which results decrease in impedance values of the specimen. The impedance values calculated from Fig.15b and Fig.16b, revealed high magnitude of resistance i.e., 1.28 x 10^9 and 2.72 x 10^9 ohms for MAS-G4 and MAS-G8 specimens respectively. Real part of permittivity (dielectric) shows the dispersion at low frequencies but at high frequency the dielectric value is least around 1.0 in both MAS glass ceramic specimens, which is according to literature (Hu et.al. 2001). It was observed that MAS-G8 glass specimen is more resistive and insulator in nature than the MAS-G4 and these result values confirmed the XRD, SEM and radiographic results of same sintered specimens.

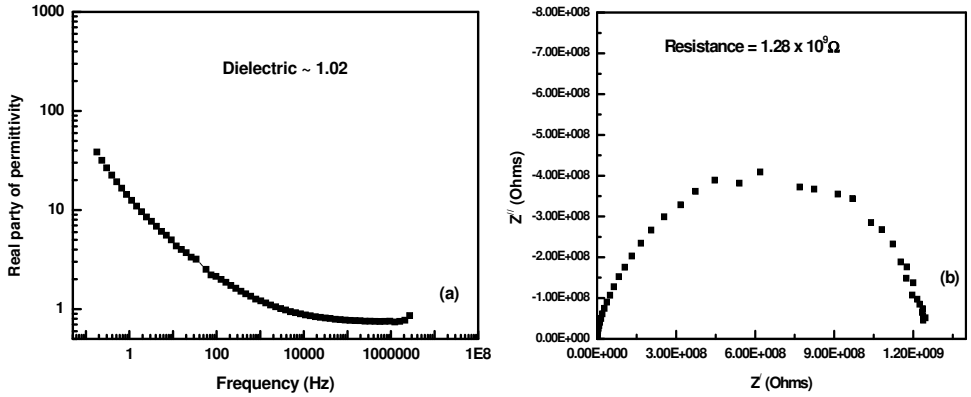

Fig. 15. Impedance analysis of MAS-G4 specimen sintered at 1050°C, (a) Variation of real part of impedance as a function of frequency in Hz (b) Impedance plane plot of MAS-G4 specimen at RT.

3.8 Effect of K_2CO_3 concentration

The physico-chemical characteristics and phase evolution during firing of MAS-K series ceramic bodies was investigated as a function of K_2CO_3 concentration and firing temperatures. The physico-chemical characteristics of sintered MAS glass specimens with variation of K_2CO_3 compositions expressed as MAS-K1- MAS-K10 and are presented in **Table 5**. Figure 15 shows the XRD patterns of MAS specimens MAS-K2-MAS-K5. The phase evolution examined by X-ray diffraction (XRD) revealed that leucite, and sillimanite are the main phases in the sintered bodies. Besides the above mentioned crystalline phases, other crystalline Mg_2SiO_4 and SiO_2 phases are also identified in Fig.16. In addition, glassy phase

fluorophlogopite appears as result of different chemical reactions during firing in some sintered MAS specimens. The relative densities (after sintering at 1040-1060°C) of MAS glass specimens were found to be decreased (85-74%) with increase of stoichiometric compositions of K_2CO_3. These stoichiometric variations altered the density, porosity and other physical properties in agreement with microstructure analyzed by SEM already shown in Fig.14(a-b), where a high fraction of porosity was observed in MAS-G10 specimen.

3.9 Influence of cooling rate after high temperature sintering treatment

MAS glass ceramic specimen (MAS-K6) was examined through cooling and quenching after high temperature sintering treatment in order to observed the influence of cooling rate on the development of phases, morphology (grain boundaries) and their impact on physical properties by studying the process of crystallization. The MAS glass ceramic (MAS-K6) specimen was heated to 1040°C, held for 4h and then cooled. The heating and cooling rates were kept 5°C/min and 5-10°C/min respectively. XRD was used to detect the developed phases on different cooing time. Figure 15 shows the XRD patterns of MAS specimen MAS-K6 (fully cooled down). The XRD data revealed that fluorophlogopite, leucite, and sillimanite are the main phases developed in the sintered bodies along with some other crystalline phases i.e. Mg_2SiO_4 and SiO_2. The observed physical characteristics, morphology and phase evolution are given in **Table 6.** It was noticed that in addition, the glassy phase, fluorophlogopite appears as result of different chemical reactions during firing and cooling. The change in density and other physical appearance were also observed due to different cooling temperatures as shown in Fig.16 (a-d). When the MAS glass material was rapid quenched after sintering exhibit silica-rich glassy phases at grain boundaries with enrichment of sillimanite, Mg_2SiO_4 and less amount of fluorophlogopite, leucite phases, Fig.16 a & f and the surface was found to be porous due to the evaporation of absorbed water. When the MAS material specimen was slowly cooled in furnace, the silica glassy phases were only present along with enrichment of fluorophlogopite and leucite phases, Fig.16 b& c.

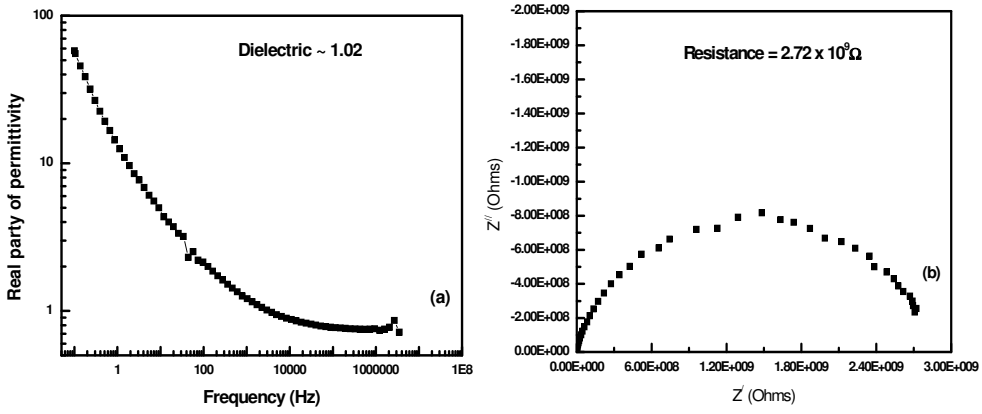

Fig. 16. Impedance analysis of MAS-G8 specimen sintered at 1040°C, (a) Variation of real part of impedance as a function of frequency in Hz (b) Impedance plane plot of MAS-G8 specimen at RT.

Specimen #	Chemical Composition (Wt %)						Firing Temperature °C	Sintered Density (g/cc)	XRD (%Phase)				Properties
	SiO_2	Al_2O_3	MgO	K_2CO_3	B_2O_3	MgF_2			F	L	S	O	
MAS-K1	43.8	17.6	16.5	12.3	5.8	4	1015	2.42	38	15	42	5	Brittle
MAS-K2	35.6	22.5	18.7	12.6	5.8	4.8	1020	2.32	34	25	29	12	Brittle and deformed
MAS-K3	47.2	12.6	16.9	14.7	5.9	4.5	1025	2.27	36	44	14	3	Brittle and swell up
MAS - K4	40.2	15.5	17.9	15.4	5.7	5.3	1030	2.34	42	12	37	9	Hard and Brittle
MAS-K5	36.4	24.7	13.5	11.4	3.6	10.4	1040	2.38	57	3	40	-	Mechinable
MAS-K6	45.3	12.4	17.1	13.7	6.8	4.7	1040	2.39	52	39	9	-	Mechinable
MAS-K7	45.5	16.8	15.9	12.6	4	5.2	1040	2.28	52	4	38	4	Mechinable
MAS-K8	37.5	20.2	17.7	12.8	5	6.8	1045	2.41	54	5	39	2	Mechinable
MAS-K9	37.5	20.2	17.7	12.8	5	6.8	1050	2.41	51	7	42	-	Mechinable
MAS-K10	38.5	16.4	19.4	11.6	7.5	6.6	1045	2.41	49	36	7	8	Hard and Brittle
MAS - K11	36.2	23.6	16.1	9.8	4	10.3	1070	2.37	46	5	40	9	Hard and Brittle

F= Fluorophlogopite L= Leucite (L) S = Sillimanite O= other phases like Mg_2SiO_4 and SiO_2

Table 5. Effect of K_2CO_3 concentration on sintered density, phase purity and physical properties of MAS glass ceramic materials.

3.10 Elemental contents

The elemental composition of prepared powder and sintered specimens of MAS-G8 glass ceramic was measured by electron probe micro analyzer (EPMA) attached with scanning electron microscope and these elemental contents were also identified by XRF. Fig. 17(a-b) shows the composition analysis of MAS-G8 specimen sintered at 1040°C estimated by EPMA and also analyzed on XRF in order to detect the contents Al, Mg, K and Si.

Physico-chemical properties	Sintering temperature =1040^{o}C				
	Specimens collected after quenching (cooling rate 10^{o}C/min).				
	1040	740	440	140	30
Density (g/cm^3)	2.05	2.19	2.34	2.31	2.28
Phase formation (%)	F= 25, L= 21 S= 48 O= 6	F= 42, L= 18 S= 31 O= 9	F= 47, L= 12 S= 37 O= 4	F= 50, L= 8 S= 37 O= 5	F= 52, L= 4 S= 38 O= 4
Characteristic	Swell up, hard and brittle	Broken , hard and brittle	Broken , hard and brittle	hard and to some extent Machinable	Machinable
Physical appearance (Shape)	Deformed, grey white color with more porosity	Deformed grey-white color with more porosity	Off-white and shining with less porosity	White with porosity (5-6%	White with porosity (5-6%)
Withdrawal of specimen conditions	After thermal treatment, specimen was taken out from the furnace and quenched in air until room temperature	After thermal treatment, specimen was remained in furnace in respective time interval. Cooling at furnace rate contemplates cutting off the electric current to the furnace and allowing the furnace to cool down for desire time and also until room temperature.			
Photographs Figure 16(a-f)	Figure 16f	Figure 16e	Figure 16d	Figure 16c	Figure 16b

F= Fluorophlogopite L= Leucite (L) S = Sillimanite O= other phases like Mg_2SiO_4 and SiO_2

Table 6. Influence of cooling rate on MAS glass ceramic specimen (MAS-K6) after high temperature sintering treatment.

3.11 Acid effect

The sintered specimens were tested for resistance to acids and bases when subjected to 5% hydrochloric acid, hydrofluoric acid at 95^{o}C for 24h for acids and 6h for sodium hydroxide and sodium carbonate bases **Table 7.** The chemical resistance i.e. weight loss per unit area (mg/cm^2) of MAS-4b either acids or base was found significant and values were found similar with (Wawrziniak et al., 1980).

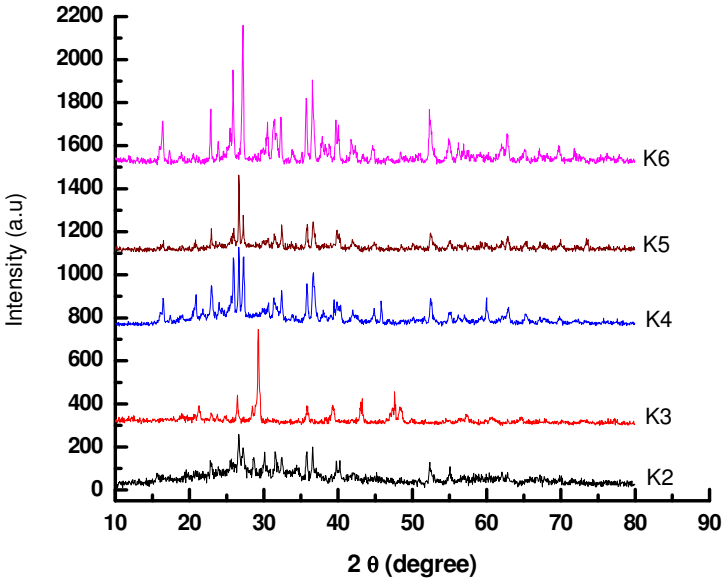

Fig. 17. XRD patterns of MAS glass ceramic specimens (MAS-K1-MASK5) as a function of variation of K_2CO_3 concentration and firing temperatures.

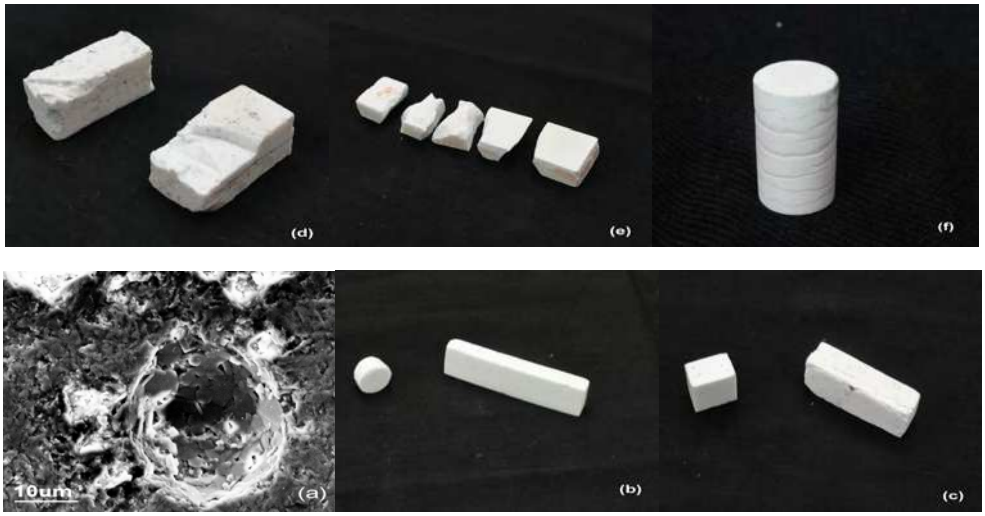

Fig. 18. (a-f): SEM image and photographs of MAS glass ceramic as a function of cooling rates after high sintering temperature (a) SEM image of MAS-K6 specimen sintered at 1040°C and cooled at 30°C (b) MAS-K6 specimen sintered at 1040°C and cooled at 30°C (c) sintered at 1040°C and cooled at 140°C (d) sintered at 1040°C and cooled at 440°C (e) sintered at 1040°C and cooled at 740°C (f) sintered at 1040°C and cooled at 1040°C.

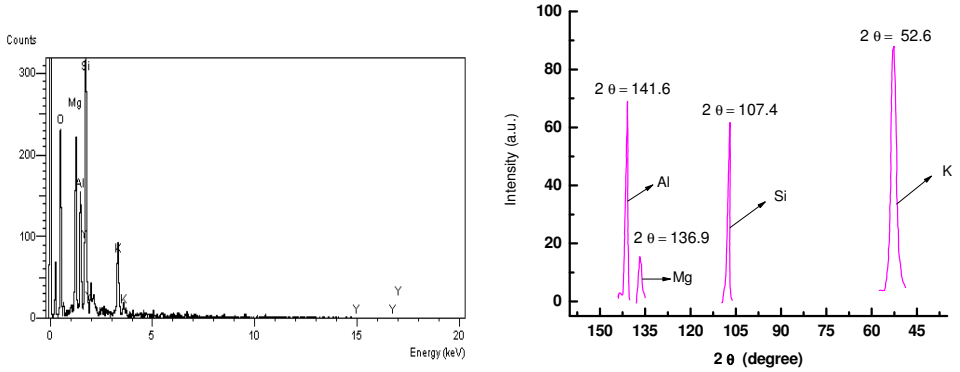

Fig. 19. (a-b): Chemical composition analysis of MAS-G8 (a) EPMA spectra (b) XRF patterns.

Specimen #	Resistance to Acid Wt-loss per unit area				Resistance to Base Wt-loss per unit area			
	Temperature °C	Time (h)	HCl (5%) (mg/cm²)	HF (5%) (mg/cm²)	Temperature °C	Time (h)	NaOH (5%) (mg/cm²)	Na_2CO_3 (5%) (mg/cm²)
MAS- G4	95	24	67	17.51	95	6	10.62	Nil
MAS- G6	95	24	87	156	95	6	9.52	2.13
MAS- G8	95	24	48	6	95	6	11.82	1.35

Table 7. Acids and bases effect on magnesium aluminum silicate glass ceramic specimens.

On the basis of experiments performed and capability for preparation of MAS glass ceramic materials using sintering route with 93% relative density contain 57% fluorophlogopite phase responsible for machinability. The high voltage insulators are required indifferent shapes and sizes so for these reasons some MAS glass ceramic materials have been developed by sintering route in different shape and size. The photographs of developed MAS glass ceramic items are as shown in Fig. 20.

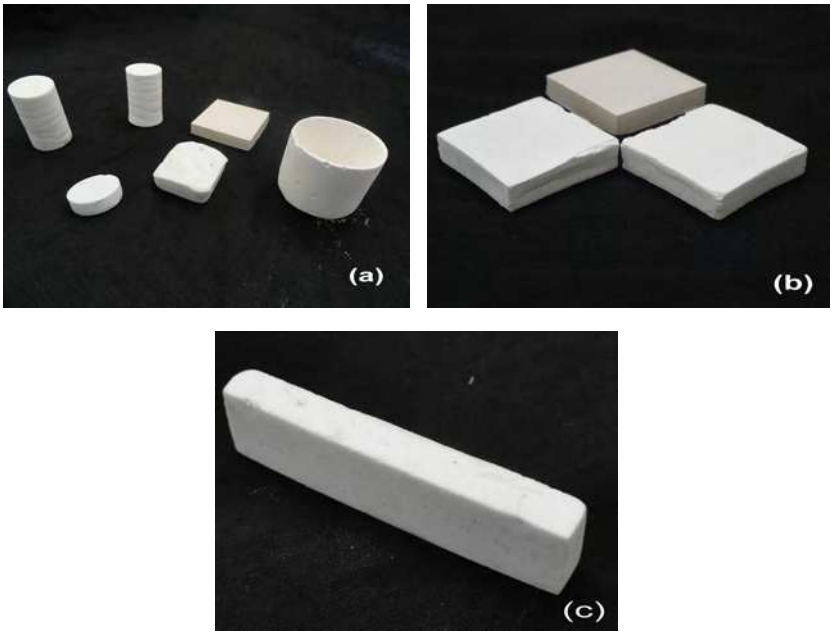

Fig. 20. (a-c): MAS glass ceramic materials in different shape and size (a) showing solid slab, cylindrical rod, green crucible, disc (b) green and sintered slabs (c) sintered rod.

4. Conclusion

Magnesium aluminum silicate (MAS) glass ceramic was prepared successfully by sintering route and characterized in terms of both phase evolution during firing and microstructure at the optimum sintering temperature. The chemical composition of specimen MAS-G8 was found appropriate as compared to other compositions. The 9.14% weight loss was observed in specimen MAS-G8 after heating up to 900°C by TG-DTA and found thermally stable above 900°C. MAS-G8 sintered at temperature 1040°C provided smaller and uniform particle size distribution, 93% theoretical density. The phase evolution examined by XRD revealed that three main phase fluorophlogopite (F), sillimanite (S) and leucite (L) were present in the prepared magnesium aluminum silicate glass ceramic specimens as result of different chemical reactions during firing; however the specimen MAS-G8 consists of predominant fluorophlogopite glassy phase with uniform particle size distribution. Radiographic studies show the least (3-4%) through porosity whereas SEM image indicates some surface porosity.

5. Acknowledgement

The authors wish to acknowledge the contributions of M. Masood, M.M.R. Baig, Zahid Hussain, Aurangzeb, M. Hussain, Zahir Ahmad, Shahid Ayub for drawing 3D figures on AutoCAD and also providing assistance during the preparation of sintered specimens, measurement of density and XRD/XRF analysis.

6. References

Abo-Mosallam, H.A.; Salama, S.N. & Salman S.M.(2009). Formulation and characterization of glass-ceramics based on $Na_2Ca_2Si_3O_9$-$Ca_5(PO_4)_3F$-Mg_2SiO_4-system in relation to their biological activity, *J. Mater. Sci. Mater*. In Med., 20, 12, (2009) 2385-2394, ISSN: 1573-4838.

Bhargava, A.K. (2005). *Engineering Materials: Polymers Ceramics and Composites,* PHI Learning Pvt. Ltd., (2005), ISBN: 8120325834, 9788120325838

Baik, D.S.; No, K.S.; Chun, J.S.; Yoon Y.Y. & Cho, H.Y.(1995). Effect of the aspect ratio of mica crystals and crystallinity on the microhardness and machinability of mica glass-ceramics, *J. Mater. Process. Tech.*, 67, 1-3, (1997) 50-54, ISSN: 0924-0136

Barsoum, M. (1994). *Fundamental of Ceramics,* McGrew-Hill, Singapore, 1997, ISBN-0-07-005521-1

Boccaccini, A.R. (1997). Machinability and brittleness of glass-ceramics, *J. Mater. Process Technol.*, 65, (1997) 302, ISSN: 0924-0136

Bapna, M. S., & Mueller, H. (1996). *J. Biomaterials,* 17, (1996) 2045-2052, ISSN: 0142-9612

Bozadzhiev L.S.; Georgiev, G.T. & Bozadzhiev, R.L.(2011) *A Glass-Ceramic Material for Fixation of Radioactive Waste, Science of Sintering,* 43, (2011) 225-229, ISSN: 0350-820X

Callister, W.D. (2010). *Materials science and engineering: an introduction*, 8th edition, John Wiley & Sons, E-Book: Wiley Desktop Edition, (2007), ISBN: 978-0-470-93281-0

Carter, C.B. & Norton, M.G. (2007). *Ceramic materials: science and engineering,* Springer, (2007), ISBN: 978-0-387-46270-7

Cattell, M.J.; Chadwick, T.C.; Knowles, J.C.; Clarke, R.L. & Samarawickrama, D.Y. (2006) *The nucleation and crystallization of fine grained leucite glass-ceramics for dental applications,* Dent.Mater., 22,10, (2006) 925-33, ISSN: 0109-5641

Chowdhury, T. (2010). *Ceramic Insulator*, VDM Verlag, Dr. Mueller E.K., (2010), ISBN: 3639306414, 9783639306415

Chen, Q. Z.; Li, Y.; Jin, L. Y.; Quinn, J. M. & Komesaroff, P. A. , A new sol-gel process for producing Na_2O-containing bioactive glass ceramics, *Acta Biomaterialia* 6, 10, (2010) 4143-4153, ISSN: 1742-7061

Ciacchi, F.T.; Crane, K.M.; & Badwal, S.P.S. (1994). Evaluation of commercial zirconia powders for solid oxide fuel cells. *Solid St. Ionics,* 73, (1994) 49-61, ISSN: 0167-2738

David E. C. & Bruce K. Zoitos(1992). Corrosion of glass, ceramics, and ceramic superconductors: principles, testing, characterization, and applications, William Andrew, (1992), ISBN: 081551283X, 9780815512837

Doremus, R.H. (1994). *Glass Science*, 2nd Edition, Jhon Wiley & Sons, (1994), ISBN:0471891746, 9780471891741

Durrani S.K.; Akhtar, J.; Ahmad, M.; M.J. Moughal M.J. (2005), *J. Mater. Sci. Technol.*, 21, 4, (2005) 563-570, ISSN 1005-0302

Durrani, S.K.; Hussain, M.A.; Hussain, S.Z.; Akhtar, J.; Saeed, A.; Hussain, N. & Ahmed, N. (2010). Fabication of magnesium aluminum silicate glass ceramics by sintering route, *Materials Science-Poland,* 28, (2010) 459, ISSN 0137-1339

Emad M El-Meliegy (2004), Machinable spodumene-fluorophlogopite glass ceramic, *Ceram. Internat.*, 30, 6, (2004) 1059-1065. ISSN: 0272-8842

German, R.M. (1996). *Sintering Theory and Practice,* Wiley-Interscience, New York, NY, (1996), ISBN-13: 978-0471057864

Goswami, M.; Sarkar, A.; Mirza, T.; Shrikhande, V.K.; Sangeeta, Gurumurthy, K.R. & Kothiyal, G.P. (2002). Study of some thermal and mechanical properties of magnesium aluminium silicate glass ceramic, *Ceram. Internat.* 28, 6, (2002) 585-592, ISSN: 0272-8842

Hattori, T.; Shigemori, A.; Mohri, J.I.; Yoshimura, M. &, Somiya, s. (1982). *Fabrication of Nonadditive Mica Ceramics by Hot Isostatic Processing,* J. Amer. Ceram. Soc. Vol. 65, 9, (1982) c142, ISSN: 1551-2916

Hench, L.L. & Wilson, J. (1993). *An Introduction to bioceramics*, World Scientific, World Scientific Publishing Co Pte Ltd. (1993), ISBN: 9789810214005

Holkova, *Z.et al.,* (2003). *Ceramics- Silikáty,* Vol. 47, (2003) 13, ISSN: 08625468

Hölland, W. & Beall, G.H. (2002). *Glass-ceramic Technology*, The American Ceramic Society, Ohio, (2002), ISBN 1-57498-107-2

Hu.J. & Qim, H. (2001). J.Magn. Magn. Mater., *231*, (2001) L1, ISSN: 0304-8853

Hussain, S.Z.; Durrani, S.K.; Hussain, M.A.;.Akhtar, J.; Saeed, A.; Hussain, N. & Ahmed, N. (2010). Phase and Thermal Analysis of Magnesium Aluminum Silicate Glass Ceramic, *J. Pak. Mate. Soc. 4,* 1, (2010), ISSN:1994-6899

Izquierdo-Barba, I.; Salinas, J. & Vallet-Regi, M. (1999). *J.Biomedical research,* 47, (1999). 243-250, ISSN: 1549-3296.

McClune, W.F. (Ed.), Powder Diffraction File, Inorganic Phaess, International Centre for Diffraction Data, 1601 Park Lane, Swarthmore, PA 19081-2389, (1987).

Koshiro, I.; Mori, K.; Miyamoto, H.; & Nanjyo, F. (1995). *4th Symposium on SOFC In Japan edited by SOFC Society of Japan,* Electrochemical Society of Japan, Tokyo, (1995) 33-40, ISSN 1344-3542

Lei, B.; Chen, X.; Wang, Y.; Zhao, N.; Miao, G.; Li, Z. & Lin, C. Fabrication of porous,bioactive glass particles by one step sintering, *Mater.Lett*. 64, 21, (2010) 2293-2295, ISSN 0167-577X

Lewis M.H.(1989). *Glasses and Glass-ceramics*, Chapman & Hall the University of Michigan, USA., (1989), ISBN : 0412276909, 9780412276903

Manfredini, T.; Pellacani, G.C.; & Rincón, J. Ma. (1997). *Glass-Ceramics: Fundamentals and Applications,* Publisher Mucchi, Modena, (1997), ISBN: 887000287X, 9788870002874

Margha, F. H.; Abdel-Hameed, S.A.M.; Ghonim, N.A.E.; Ali, S.A.; Kato, S.; Satokawa, S. & Kojima, T. (2009). Crystallization behaviour and hardness of glass ceramics rich in nanocrystals of ZrO_2, *Ceram. Internat.* 35, I3, (2009) 1133-1137, ISSN: 0272-8842

Michael, B. (2007). Barium lanthanum silicate glass-ceramics, *US Patent 7189668,* 2007.

Miller, R. & Miller, M. R.(2002), *Electronics the Easy Way*, Barron's Educational Series, (2002), ISBN: 0764119818, 9780764119811

Minh, N.Q. & Takahashi, T (1995). *Science and Technology of Ceramic Fuel Cells,* Elsevier, Amsterdam, (1995), ISBN 13: 978-0-444-89568-4.

Mitchell, B.S.(2004) *An introduction to materials engineering and science for chemical and materials engineers,* Wiley-IEEE, (2004), ISBN: 0471436232, 9780471436232

Moghadam F.K. & Steveson, D. A. (1982). *J. Amer., Ceram. Soc.,* 65, (1982), 213-15, ISSN: 1551-2916

Montedo O. R. K.; Floriano, F.J.; Filho, J. O.; Angoletto E. & Bernardin A.M. (2009). Sintering behavior of LZSA glass-ceramics, *Mater. Res*. 12, (2009), 197-200, ISSN: 1516-1439

Mostaghaci, H. (1996). *Advanced ceramic materials: applications of advanced materials in a high-tech society* , Trans Tech Publications, (1996), ISBN : 0878497455, 9780878497454

Moulson A.J. & Hebert J.M. (1992). *ElectroCeramic Materials Properties Application,* Chapman & Hall, New York, NY 10001, USA, (1992), ISBN 0471 49748 7

Novaes de Oliveira A.P.; Manfredini T.; Leonelli C. & Peellacani, G. C.(1994). Physical Properties of Quenched Glasses in the Li_2O-ZrO_2-SiO_2 System *J. Amer. Ceram. Soc.,* 79, (1994) 1092-1094, ISSN: 1551-2916

Olevsky,E.A.; Bordia, R.(2009) *Advances in Sintering Science and Technology,Vol.211,Ceramic Transactions Series,* John Wiley & Sons, (2009), ISBN: 0470408499, 9780470408490

Pannhorst, W. (1997). Glass ceramics: State-of-the-art, *J. Non. Cryst, Solids.* 219 (1997) 198-204, ISSN 0022-3093

Partridge, G. (1994). An overview of glass-ceramics. Part. 1. Development and principal bulk applications. *Glass Technol.*, 35, (1994), 116-127, ISSN 0017-1050

Perdomol, F.; Avaca, L. A.; Aegerter, M. A. & Lima-Neto, P. De.(1998). *J. Mater. Sci. Lett.* 17, (1998) 295, ISSN 0261-8028

Radojic, L.J. & Nikolic, L.J. (1991). *Eur. Ceram. Soc.* 7, (1991) 11, ISSN: 0955-2219

Rahaman, M.N. (2003). *Ceramic Processing and Sintering,* 2nd Ed. Vol. 23. New York: Taylor & Francis, Inc., (2003), ISBN-13: 978-0824709884

Rajendran, V. (2004). *Materials Science,* Tata McGraw-Hill Education, (2004), p.40-44, ISBN: 0070583692, 9780070583696

Rice, R. & Rice, W. (2002) *Ceramic Fabrication Technology, Volume 20, Materials engineering* CRC Press, (2002), ISBN:0824745736, 9780824745738

Richerson, D.W. (1992). *Modern Ceramic Engineering: Properties, Processing and Use in Design,* 2nd Ed. New York: Marcel Dekker, (1992), ISBN-13: 978-0824786342

Rincón, J. Ma. (1992). Principles of Nucleation and Controlled Crystallization of Glasses. *Polym. Plast. Technol. Eng.,* 3, (1992) 309-357, ISSN: 0360-2559

Ring, T.A. (1996). *Fundamentals of ceramic powder processing and synthesis,* Academic Press, (1996), ISBN: 0125889305, 9780125889308

Roy, S. & Basu.B. (2006). *Microstructure Development in Machinable Mica Based Dental Glass Ceramics.* Trends in Biomaterials and Artificial Organs, Vol.20, No.(1), (2006) 90-100, ISSN 0971-1198

Shackelford, J. F. & Doremus R.H. (2008). *Ceramic and glass materials: structure, properties and processing,* Springer, (2008), ISBN 0387733612, 9780387733616

Shinroku, S. (1987). *Fine Ceramics*, Elsever Science Publishing, Co.,Vanderbilt Avenue, New York, USA. (1987), ISBN-13: 978-0444011930

Simmons, J.H.; Uhlmann D.R. & Beall G.H. (1982), *Nucleation and crystallization in glasses,* American Ceramic Society, 1982 Science, ISBN: 060800720X, 9780608007205

Smothers, .W (2009) *5th Annual Conference on Composites and Advanced Ceramic Materials: Ceramic Engineering and Science Proceedings, Volume 2, Issues 7-8,* Wiley & Sons John Wiley & Sons (2009) , ISNB:0470291516, 9780470291511

Steffestun, B. & Frischat, G.H. Alkali-Resistant Magnesium Aluminosilicate Oxynitride Glasses. J. Am. Ceram. Soc. 76 (1993), 699-704, ISSN: 1551 2916

Strnad, Z. (1986). *Glass Ceramic materials:: liquid phase separation, nucleation, and crystallization in glasses,* Elsevier, Amsterdam, (1986),ISBN: 0444995242, 9780444995247

Swab, J.J. (2009). *Advances in ceramic armor V: ceramic engineering and science proceedings.* I5, Vol.30, John Wiley and Sons, (2009), ISBN: 0470457554, 9780470457559

Ting, J. M. & Lin, R.Y. Effect of particle size distribution on sintering, *J. Mater. Sci.* 30, (1995) 2382-2389, ISSN 0022-2461

Valenzuela, R., (2005). *Magnetic Ceramics*, Cambridge University Press, (2005) ISBN: 0521018439, 9780521018432

Yuan, Q..L.; Zhang, P.; Gao, L.; Peng, H.; Ren, X. & Zhang, D.(2010). MgO-Al_2O_3-SiO_2 Glass-Ceramic Prepared by Sol-Gel Method, *Advan. Mater. Res.* 92, (2010) 131-137, ISSN: 1022-6680

Yu, Y., Wang, X., Cao, Y. & Hu, X., *Appl. Surf. Sci.,* 172, 3-4, (2001) 260-264, ISSN: 0169-4332

Wang. Y., (2008). *Introduction to ceramics,* McGraw-Hill Education (Asia), (2008), ISBN: 0071274979, 9780071274975

Wawrziniak,W. & Grunov, r. (1980). *Silikat technik,* 31, (1980) 238, ISSN: 0037-5233.

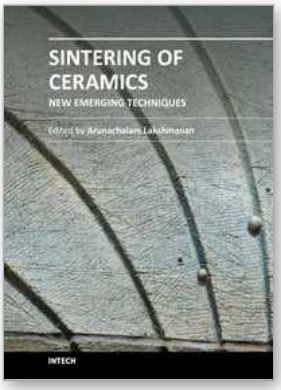

Sintering of Ceramics - New Emerging Techniques
Edited by Dr. Arunachalam Lakshmanan

ISBN 978-953-51-0017-1
Hard cover, 610 pages
Publisher InTech
Published online 02, March, 2012
Published in print edition March, 2012

The chapters covered in this book include emerging new techniques on sintering. Major experts in this field contributed to this book and presented their research. Topics covered in this publication include Spark plasma sintering, Magnetic Pulsed compaction, Low Temperature Co-fired Ceramic technology for the preparation of 3-dimesinal circuits, Microwave sintering of thermistor ceramics, Synthesis of Bio-compatible ceramics, Sintering of Rare Earth Doped Bismuth Titanate Ceramics prepared by Soft Combustion, nanostructured ceramics, alternative solid-state reaction routes yielding densified bulk ceramics and nanopowders, Sintering of intermetallic superconductors such as MgB2, impurity doping in luminescence phosphors synthesized using soft techniques, etc. Other advanced sintering techniques such as radiation thermal sintering for the manufacture of thin film solid oxide fuel cells are also described.

InTech Europe
University Campus STeP Ri
Slavka Krautzeka 83/A
51000 Rijeka, Croatia
Phone: +385 (51) 770 447
Fax: +385 (51) 686 166
www.intechopen.com

InTech China
Unit 405, Office Block, Hotel Equatorial Shanghai
No.65, Yan An Road (West), Shanghai, 200040, China
中国上海市延安西路65号上海国际贵都大饭店办公楼405单元
Phone: +86-21-62489820
Fax: +86-21-62489821